

High resolution Fourier domain optical coherence tomography in the 2 μm wavelength range using a broadband supercontinuum source

C. S. Cheung,¹ J. M. O. Daniel,^{2,3} M. Tokurakawa,^{2,4} W. A. Clarkson,² and H. Liang^{1,*}

¹*School of Science & Technology, Nottingham Trent University, Nottingham NG11 8NS, UK*

²*Optoelectronics Research Centre, University of Southampton, Highfield, SO17 1BJ, UK*

³*Present address: Aether Photonics, Melbourne, Australia*

⁴*Present address: Institute for Laser Science, University of Electro-Communications 1-5-1 Chofugaoka, Chofu-shi, Tokyo 182-8585, Japan*

*Haida.Liang@ntu.ac.uk

Abstract: A 220 nm bandwidth supercontinuum source in the two-micron wavelength range has been developed for use in a Fourier domain optical coherence tomography (FDOCT) system. This long wavelength source serves to enhance probing depth in highly scattering material with low water content. We present results confirming improved penetration depth in high opacity paint samples while achieving the high axial resolution needed to resolve individual paint layers. This is the first FDOCT developed in the 2 μm wavelength regime that allows fast, efficient capturing of 3D image cubes at a high axial resolution of 13 μm in air (or 9 μm in paint).

©2015 Optical Society of America

OCIS codes: (110.4500) Optical coherence tomography; (120.3180) Interferometry; (290.4210) Multiple scattering; (320.6629) Supercontinuum generation; (140.3070) Infrared and far-infrared lasers.

References and links

1. D. Huang, E. A. Swanson, C. P. Lin, J. S. Schuman, W. G. Stinson, W. Chang, M. R. Hee, T. Flotte, K. Gregory, C. A. Puliafito, and J. G. Fujimoto, "Optical coherence tomography," *Science* **254**(5035), 1178–1181 (1991).
2. D. Stifter, "Beyond biomedicine: a review of alternative applications and developments for optical coherence tomography," *Appl. Phys. B* **88**(3), 337–357 (2007).
3. H. Liang, M. G. Cid, R. G. Cucu, G. M. Dobre, A. Podoleanu, J. Pedro, and D. Saunders, "En-face Optical Coherence Tomography - a novel application of non-invasive imaging to art conservation," *Opt. Express* **13**(16), 6133–6144 (2005).
4. H. Liang, B. Peric, M. Hughes, A. Podoleanu, M. Spring, and S. Roehrs, "Optical Coherence Tomography in Archaeology and Conservation Science – A new emerging field," *Proc. SPIE* **7139**, 713915 (2008).
5. P. Targowski and M. Iwanicka, "Optical Coherence Tomography for structural examination of cultural heritage objects and monitoring of restoration processes – a review," *Appl. Phys. A* **106**(2), 265–277 (2012).
6. H. Liang, R. Lange, B. Peric, and M. Spring, "Optimum spectral window for imaging of art with optical coherence tomography," *Appl. Phys. B* **111**(4), 589–602 (2013).
7. B. E. Bouma, L. E. Nelson, G. J. Tearney, D. J. Jones, M. E. Brezinski, and J. G. Fujimoto, "Optical coherence tomography imaging of human tissue at 1.55 μm and 1.81 μm using Er- and Tm-doped fiber sources," *J. Biomed. Opt.* **3**(1), 76–79 (1998).
8. U. Sharma, E. W. Chang, and S. H. Yun, "Long-wavelength optical coherence tomography at 1.7 μm for enhanced imaging depth," *Opt. Express* **16**(24), 19712–19723 (2008).
9. S. Ishida and N. Nishizawa, "Quantitative comparison of contrast and imaging depth of ultrahigh-resolution optical coherence tomography images in 800-1700 nm wavelength region," *Biomed. Opt. Express* **3**(2), 282–294 (2012).
10. H. Kawagoe, S. Ishida, M. Aramaki, Y. Sakakibara, E. Omoda, H. Kataura, and N. Nishizawa, "Development of a high power supercontinuum source in the 1.7 μm wavelength region for highly penetrative ultrahigh-resolution optical coherence tomography," *Biomed. Opt. Express* **5**(3), 932–943 (2014).
11. C. S. Cheung, M. Tokurakawa, J. M. O. Daniel, W. A. Clarkson, and H. Liang, "Long wavelength optical coherence tomography for painted objects," *Proc. SPIE* **8790**, 87900J (2013).
12. C. S. Cheung, J. M. O. Daniel, M. Tokurakawa, W. A. Clarkson, and H. Liang, "Optical coherence tomography in the 2- μm wavelength regime for paint and other high opacity materials," *Opt. Lett.* **39**(22), 6509–6512 (2014).

13. A. Fercher, C. Hitzenberger, G. Kamp, and S. El-Zaiat, "Measurement of intraocular distances by backscattering spectral interferometry," *Opt. Commun.* **117**(1-2), 43–48 (1995).
14. J. M. O. Daniel and W. A. Clarkson, "Bandwidth-Controllable Tunable Q-Switched Thulium Fibre Laser," European Conference on Lasers and Electro-Optics, CJ-10.2 THU (2013).
15. J. M. Dudley and J. R. Taylor, eds., "Supercontinuum generation in optical fibers," (Cambridge University Press, 2010).
16. A. Lerwill, A. Brookes, J. Townsend, S. Hackney, and H. Liang, "Micro-fading spectrometry: investigating the wavelength specificity of fading," *Appl. Phys. A Mater. Sci. Process.* (2015), doi:10.1007/s00339-014-8645-3.
17. A. Szkulmowska, M. Góra, M. Targowska, B. Rouba, D. Stifter, E. Breuer, and P. Targowski, "Applicability of optical coherence tomography at 1.55 μm to the examination of oil paintings," In *Lasers in the Conservation of Artworks*, Springer proceedings in Physics. **116**, 487–492 (2007).
18. N. Nishizawa, "Generation and application of high quality supercontinuum sources," *Opt. Fiber Technol.* **18**(5), 394–402 (2012).

1. Introduction

Optical Coherence Tomography (OCT) is a non-invasive and non-contact technique for rapid 3D imaging of subsurface microstructure of materials that are transparent or semi-transparent in the near infrared. It was first designed for the in vivo examination of the eye [1]. OCT is increasingly being used for a variety of applications including non-biological applications [2]. The application of OCT to cultural heritage is a relatively recent [3] but fast growing area of research [4,5]. While current OCTs have shown potential in this field, they are optimized for biomedical applications. One major shortcoming is the limited probing depth through highly scattering paint.

Increasing the probing depth needs light sources at longer wavelength than conventionally used in biomedical imaging. A recent survey of the transparency of historical artists' pigments over the spectral range of 400 nm – 2400 nm has shown that the optimum spectral window for OCT imaging of paint layers is around 2200 nm [6]. Off-the-shelf OCT sources are commonly found around 800 nm, 1000 nm, 1300 nm and 1500 nm and few OCT systems have been built beyond 1300 nm. Development of OCT devices in the 2 μm wavelength regime requires development of broadband sources.

There have been very few developments of long wavelength OCT beyond 1.5 μm [7–12]. We have previously demonstrated through a time-domain OCT system the significantly improved probing depth of long wavelength OCT in comparison to short wavelength sources [11, 12]. This system, based on a 40 nm bandwidth 1960 nm amplified spontaneous emission (ASE) source, is capable of revealing layer structures of paints, such as Titanium white and Prussian blue, that are normally opaque for OCT at 1550 nm, 1300 nm and 930 nm. However, due to the relatively narrow bandwidth of the source and the long acquisition times associated with time-domain OCT, it was limited in axial resolution (~ 35 microns) and speed.

In this paper, we demonstrate an improved system using a broadband supercontinuum source with more than 5 times wider bandwidth. In addition to this, we adopt a Fourier domain OCT (FDOCT) configuration [13], greatly improving the acquisition speed of the system.

2. High stability supercontinuum generation at two microns

The coherence length of the light source used within an OCT system determines the achievable axial resolution which for a Gaussian shaped spectrum is given by $\sim 0.44\lambda_0^2/\Delta\lambda$ where λ_0 is the central wavelength of the source and $\Delta\lambda$ is the full width at half maximum (FWHM) bandwidth. To achieve an axial resolution of ~ 10 μm , a 2000 nm OCT system needs to have a source bandwidth of ~ 180 nm which is generally beyond what is readily achievable for semiconductor or rare earth doped laser sources. In this work, we push beyond the gain bandwidth of Thulium doped fiber sources by taking advantage of non-linear supercontinuum generation. An in-house built high peak power pulsed source is used to generate broadband supercontinuum (SC) light directly within the wavelength range of interest.

2.1 Experimental arrangement

Following a modified arrangement to that reported in [14] a pulsed seed source was constructed around a 1.2 m length of thulium doped active fiber (0.2 wt % Tm concentration), having a core diameter of 10 μm , NA of ~ 0.13 and an estimated single mode cut-off at ~ 1700 nm. The outer cladding diameter of this fiber was 100 μm . Pump light was provided by a single mode 1565 nm fiber laser source and was launched into the core of the thulium fiber via a wavelength division multiplexer (WDM). Up to 4 W of pump power was coupled into the active fiber. A simple linear arrangement was adopted for this pulsed source with an external cavity containing an acousto-optic modulator (AOM) and highly reflective mirror providing modulated feedback. Rise and fall times of this AOM were measured to be ~ 70 ns (10–90% points). Laser output was taken after a fiberized isolator. Initially designed for use at 2000 nm, the internal back-reflection of this isolator was found to provide sufficient feedback to the Q-switched source to generate stable output pulses and enabled a pigtailed, isolated output that could later be easily spliced to the continuum generating fiber. When pulsed, the source operated with a peak wavelength of 1850 nm and a broad spectral output of 24 nm FWHM. Pulse repetition rate could be tuned from 10 kHz to 200 kHz, limited by parasitic lasing at the lower repetition rates and pulse skipping at the higher repetition rates. Maximum pulse energy at maximum pump power occurred at a pulse repetition rate of 25 kHz with pulse energy of 39 μJ and width of 50 ns, corresponding to average and peak laser output powers of 0.98 W and 0.78 kW respectively. At a repetition rate of 50 kHz, the average power is ~ 1.2 W, the pulse energy is 23 μJ and the pulse duration is ~ 100 ns.

The single mode output from this pulsed source was directly spliced onto a 5 m length of small-core germanium-doped, highly nonlinear fiber (HNLF) and was used as a seed source to initiate continuum generation. This HNLF was fabricated by Fibercore, having an estimated germanium doped core diameter of 3.8 μm and NA of 0.29. The cut-off wavelength of 1400 nm, zero dispersion point of 1550 nm and mode field diameter of 5.30 μm (at $\lambda = 1850$ nm) were calculated using commercially available mode solving software (Optifiber). Hence this fiber showed anomalous dispersion and single mode propagation across the entire wavelength range of interest.

After optimization, splice loss between the Q-switched source (SMF28e) and the HNLF was reduced to $\sim 15\%$. Resulting in a maximum peak power of ~ 0.67 kW launched into the HNLF. This corresponded to a total launched seed power of 835 mW (at a pulse repetition rate of 25 kHz). The experimental layout of this supercontinuum source is shown in Fig. 1.

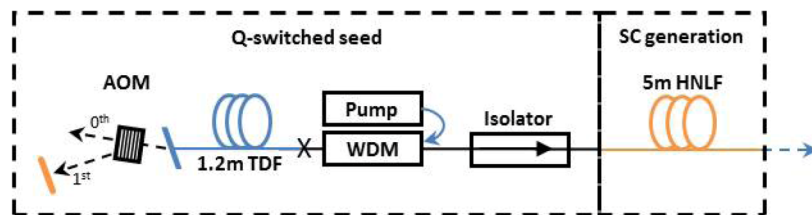


Fig. 1. Experimental layout of the supercontinuum source. AOM: acousto optic modulator. TDF: thulium doped fibre. WDM: wavelength division multiplexer. HNLF: highly nonlinear fibre.

2.2 Characteristics of the supercontinuum source

At a 25 kHz pulse repetition rate and ~ 0.67 kW of launched peak power, the HNLF produced a supercontinuum output ranging from 1800 nm through to 2300 nm with the bulk of the continuum generation occurring at wavelengths longer than the 1850 nm seed. For 835 mW of launched seed power, 637 mW of supercontinuum output was generated, with a spectral power density of > 0.5 mW/nm over a 400 nm wavelength range from ~ 1800 nm – 2200 nm. The level of pulse-to-pulse spectral fluctuation both on a pulse-to-pulse basis and over an extended time period determines the suitability of the source for OCT application. We

measured the spectrally dependent pulse-to-pulse energy variations of this supercontinuum source through use of a high-resolution monochromator and fast photodiode. A small area InGaAs photodiode with temporal bandwidth of 50 MHz was used for the pulse-to-pulse stability measurements including the direct measurement of spectrally dependent pulse-to-pulse fluctuations. A spectral selectivity of ~ 3 nm was obtained with the monochromator and detector arrangement. The standard deviation of pulse energy was measured across the emission band and found to be less than 1% across the entire wavelength range of interest. These values show deterioration from the initial seed stability of 0.15%.

Owing to the pump wavelength being within the anomalous dispersion regime and the relatively long pulse width, the continuum generation is expected to be initiated by the onset of modulation instability within the HNLF [15]. Here a pulse break-up of the initial 50 ns pulse into a large number of picosecond duration solitons occurs, which can explain the relatively smooth spectra and high pulse-to-pulse stability. Although the formation of a single soliton in this picture is highly unpredictable, the relatively long pulse width of the pump in comparison with the modulation instability period of the fiber (of the order of 1ps) results in a very large number of solitons being formed within the pulse envelope. Owing to statistical averaging, the result is stable supercontinuum generation within the original pulse envelope as found in the spectral dependent pulse measurements. Longer term stability measurements were conducted on this source through the comparison of several time averaged spectral measurements (using an optical spectral analyzer) taken at half-hour intervals. With the generated spectral shape compared across an hour-long timescale, we found $\sim 5\%$ ($\pm 2.5\%$) variation in spectral shape. These variations are suspected to be a result of temperature drift of external cavity components within the pulsed seed source. By moving to an all fiberized seed it is expected that the long term source stability can be further improved.

3. Fourier domain OCT system at 2 μm

A fiber-based Fourier domain OCT system as shown in Fig. 2 was constructed from this supercontinuum source. Prior to launching into the FDOCT arrangement, the supercontinuum output was passed through a length of un-pumped thulium doped fiber which served as a soft cut-on long pass filter ($> \sim 1850\text{nm}$) to remove the pump emission. This spectral filtering process reduces the output power by $\sim 50\%$.

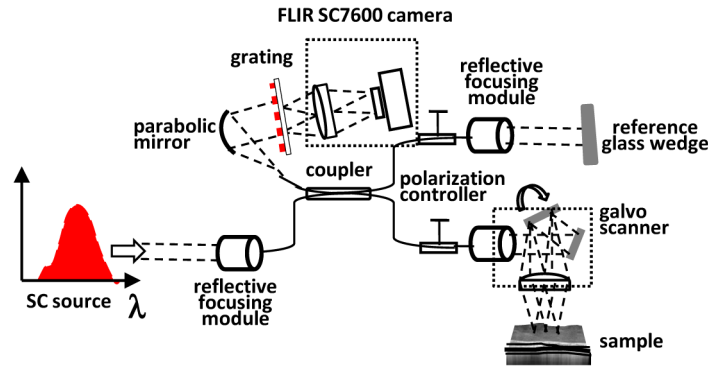


Fig. 2. Schematic diagram of Fourier domain OCT at 2 microns

This spectrally filtered supercontinuum source was then coupled into the input arm of a 2 μm fiber coupler (Gooch & Housego). The light is split into a reference and a sample arm. In the sample arm, light is directed onto galvo scanning mirrors which scan and collect the returning light from the sample. The light reflected back from a fixed glass wedge in the reference arm mixes with the signal returned from the sample arm. This interference signal in the output arm of the fiber coupler is dispersed through a transmission grating with 300 lines/mm (Thorlabs GTI25-03A) and the wavelength range between 1840 and 2200nm is detected by a 14bit InSb camera (FLIR SC7600) with 640 by 512 pixels (pixel size 15

microns). The maximum frame rate of the camera is 2750 Hz for a 640 by 4 pixel subframe (minimum allowed subframe as defined by camera hardware). The choice of the FLIR InSb camera rather than a linear 1024 pixel extended InGaAs camera is the greater sensitivity offered by the InSb detector in this wavelength range. A matching camera lens (FLIR L0608T f/3, $f = 50\text{mm}$, transparent in the $1.5\text{--}5\ \mu\text{m}$ spectral region) is used to focus the light from the grating to the detector. A short pass filter is used to block out unwanted thermal emission at wavelengths greater than $2.6\ \mu\text{m}$. Given the limited availability of components in the $2\ \mu\text{m}$ wavelength regime as well as the challenges associated with such a broad spectral range, reflective optics were used where possible to avoid chromatic aberration. The spot size of the light focused on the detector is measured to be <2 pixels ($<30\ \mu\text{m}$) and hence 2 rows of 640 pixels were averaged to produce a spectrum.

Spectral calibration using lamps with standard emission lines is difficult in this wavelength regime because of the lack of strong and narrow emission lines. Instead a glass slide of known thickness was used to calibrate the system. The spectrum was then resampled into uniform k -space, zero padded and Fourier transformed into a depth profile.

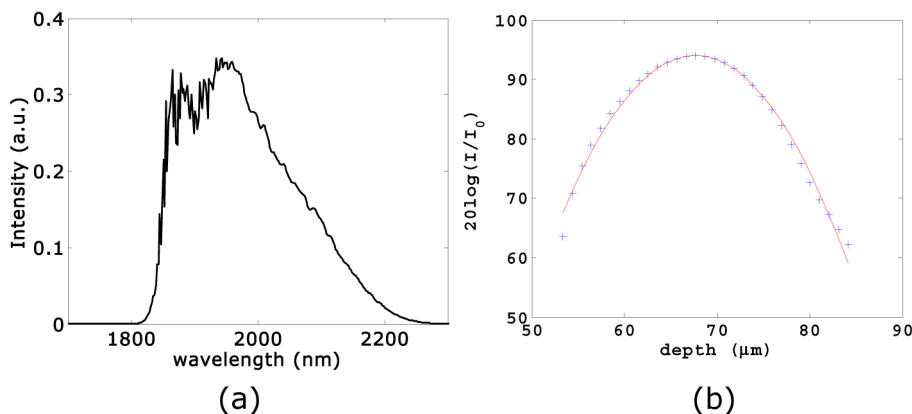


Fig. 3. a) Spectrum of the supercontinuum source output after spectral filtering with an unpumped section of thulium doped fiber; b) OCT depth profile through a glass surface; the red curve is a Gaussian of $13\ \mu\text{m}$ FWHM and the blue crosses are measured values.

The SC source was operated at a repetition rate of 50 kHz for the desired incident power on the sample. The final spectrum from the source output is shown in Fig. 3(a) where the central wavelength is at 1960 nm and the FWHM bandwidth is 220 nm. The OCT theoretical axial resolution is $\sim 11\ \mu\text{m}$ derived from simulations using the actual source spectrum, the detector spectral response and assuming that all other components have a flat spectral response. The spectral response of the fiber coupler was not taken into account in these simulations though it may have an effect on the final spectral shape and bandwidth due to non-uniform coupling ratio across the SC bandwidth. However, the experimentally measured axial resolution of this system in air was $\sim 13\ \mu\text{m}$ (Fig. 3b) which is consistent with our simulation, suggesting variations in coupling ratio had only minimal adverse effect on the resolution. It was interesting that even with such a broadband source, there was no need for dispersion compensation between the two arms in this wavelength regime even though the fiber lengths were not exactly equal and different optical components were used in the two arms. The transverse resolution of the OCT is determined by the objective lens and found to be $\sim 17\ \mu\text{m}$ by scanning a USAF microscope resolution standard.

Due to the relatively low repetition rate of this SC source, pulse frequency must be taken into account. This is in contrast to commercially available mode locked supercontinuum sources that tend to operate at MHz repetition rates and can generally be treated as pseudo continuous-wave sources. It is therefore important to synchronize the camera exposure and frame rate to the SC pulse duration and frequency. A camera frame rate of 2.5 kHz means the interval between two successive A-scans corresponds to the duration of exactly 20 pulses for

a source repetition rate of 50 kHz. If the frame rate of the camera can be adjusted to the SC source repetition rate, then the total light energy incident on a sample can be greatly reduced. The clocking signal that controls the SC repetition rate is frequency down-converted from 50 kHz to 2.5 kHz to trigger the camera capture such that the camera exposure is synchronized with the pulse arrival. Ideally for maximum signal-to-noise ratio, it is best to have the camera exposure time equal to the pulse width, since only noise will be captured during the ‘dead time’ between pulses. However, the minimum possible camera exposure time is 1 μ s (10 times greater than the pulse full width) and exposure times are only accurate to 250 ns. In addition, the camera capture timing uncertainties are significant for exposure times less than 5 μ s and hence limiting the minimum reliable synchronized (with the pulses) exposure times to 6 μ s. On the other hand, the readout noise of this camera dominates over the exposure time dependent dark current noise and therefore this longer exposure time does not reduce the signal-to-noise ratio significantly.

Visibility is a maximum when the returned signals from the two arms are equal. To estimate the sensitivity of the system, a glass microscope slide was imaged and the air/glass interface at the focus position was 95 dB while the noise level in the absence of a sample was found to be 35 dB. Since the reflectivity of the air/glass interface at normal incidence is \sim 4% (i.e. 28 dB below a 100% reflective surface such as a mirror), the sensitivity of the system is therefore -88 dB (i.e. 0.006% reflectivity) for an incident power of 1.3 mW on the sample.

4. FDOCT Imaging of paint samples at 2 microns

The OCT incident power used for imaging paint samples was kept at \sim 1 mW to avoid light induced degradation. This incident power over a typical \sim 10-20 micron spot size is used in general for biomedical application as well as imaging of paintings at the usual OCT wavelength of 800-1300 nm. Light induced degradation is usually greatest at UV and blue regions of the spectrum due to the larger photon energy; and wavelength range corresponding to strong absorption of the material. Photo-degradation reduces with wavelength since these materials are more transparent at longer wavelength [6]. Using the results from light-induced accelerated ageing experiments using broadband sources with an approximate daylight spectrum (400-700 nm) of some of the most sensitive pigments such as Prussian blue [16], we can deduce that an OCT operating at 1 mW over a spot size of 17 μ m in diameter with an exposure time of 6 μ s is at least 4 orders of magnitude below the damage threshold even if the OCT uses a source with the same visible spectrum.

Figure 4 shows an example of an application to paint imaging using a mock-up historical paint sample. The sample was prepared on a Teflon board sized with a ground layer of chalk in rabbit skin glue. The left half of the board is painted with a dark blue smalt (ground cobalt glass) pigment in linseed oil and the right half is painted with a yellow ochre pigment in linseed oil. A thin mastic varnish layer is then applied above the paint layers. While the 930 nm FDOCT (Thorlabs, axial resolution 6.5 μ m) reveals the smalt layer and the thin varnish layer above the yellow ochre paint, it does not show the interface between the yellow ochre paint layer and the chalk ground except perhaps near the boundary between yellow ochre and smalt where the yellow ochre layer is thin (Fig. 4b). Multiple scattering masks the yellow ochre paint/chalk ground interface at 930 nm. However, the FDOCT at 1960nm was able to reveal clearly the interface between the yellow ochre paint and the chalk ground while still resolving the thin varnish layer on top of the yellow ochre paint (Fig. 4c). Yellow ochre is known to be highly scattering with scattering coefficient decreasing with increasing wavelength [6] and an OCT examination at 1550 nm of yellow ochre oil paint layer found it to be dominated by multiple scattering [17]. While the smalt paint/chalk ground interface can be seen in the 1960 nm OCT image, it is not as clear as that in the 930 nm OCT image. Smalt is one of the very few pigments that is more transparent at 930 nm than at 2 μ m [6]. The stronger absorption of smalt at 2 μ m results in reduced number of photons reaching the chalk layer. This example shows that the improved resolution of this 2 μ m OCT over our previous ASE source based OCT [11,12] allows thin varnish and paint layers to be resolved while

increasing the probing depth in highly scattering paint compared with shorter wavelength OCT.

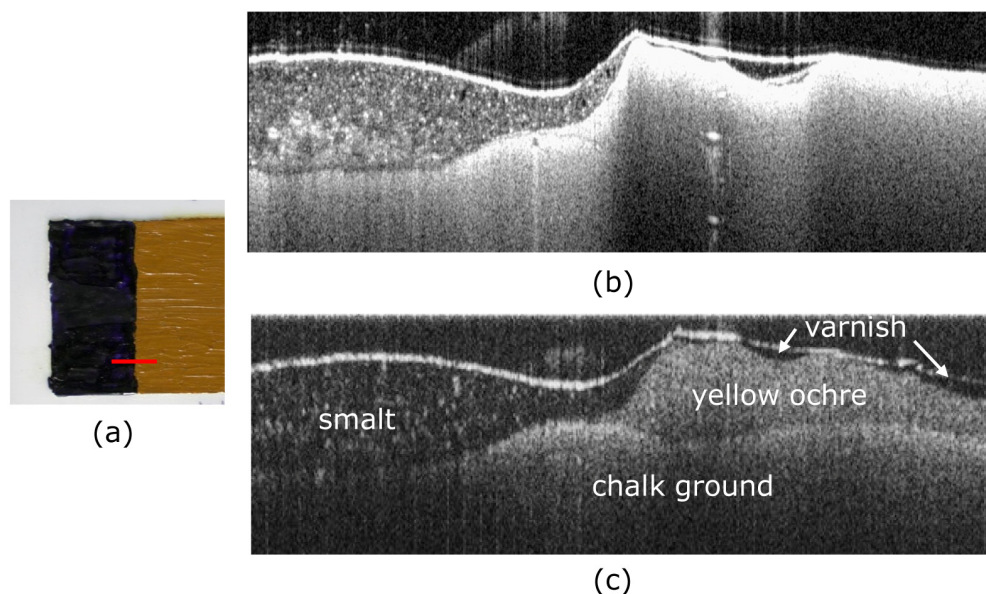


Fig. 4. a) Color image of smalt (left) and yellow ochre (right) in linseed oil painted on a Teflon board prepared with a ground layer of chalk in rabbit skin glue; there is a thin mastic varnish layer on top of the paint layers; b) 930nm FDOCT B-Scan in the region marked with a red line segment in a); the very faint line above the brightest interface is a sidelobe artefact; c) high resolution 1960nm FDOCT B-Scan at roughly the same position. B-Scan image sizes are 7 mm wide by 0.8 mm deep.

Figure 5 shows an example of the 1960nm OCT for imaging underdrawings below paint layers that contain paint that are considered to be strongly scattering (e.g. lead white) and strongly absorbing (e.g. malachite) in the usual visible and very near infrared range. Direct imaging of the sample in the spectral window of $\sim 1500\text{-}1650\text{ nm}$ (Fig. 5b) did not reveal any underdrawing, while direct imaging in the spectral range $\sim 1500\text{-}2500\text{ nm}$ showed a very faint underdrawing signal (Fig. 5c). Figure 5(d) shows the superior contrast and resolution of the OCT 'en face' image at 1960nm compared with direct imaging in a similar wavelength range using the same FLIR SC7600 InSb camera (Fig. 5c) as that used in the spectrograph of the OCT. The OCT 'en face' image of the underdrawing in Fig. 5(d) is an average of 'en face' slices that contained the underdrawings, that is the slices above the underdrawings were excluded. The depth resolved imaging capability as well as the high dynamic range and resolution imaging offered by interferometry enables OCT to produce the best images of underdrawings. The improved speed of capture of this FDOCT by more than 20 times compared with the previous TDOCT means that imaging of underdrawings that typically requires 3D volume scans are more efficient and practically possible. The collection of the image cube that produced Fig. 5d took 3 minutes.

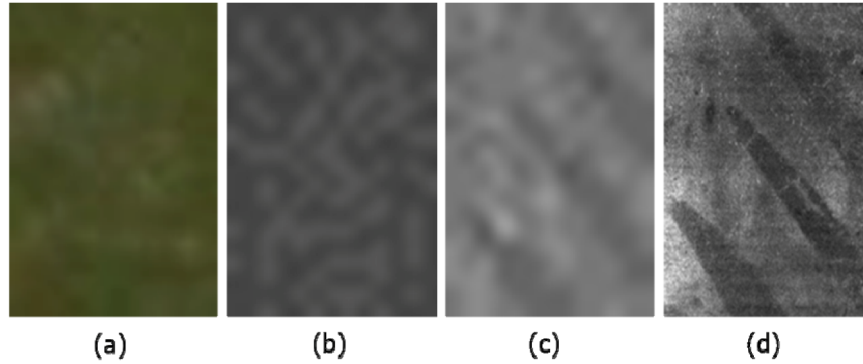


Fig. 5. a) Color image of a paint sample consisting of two bottom layers of a mixture of malachite, lead white and buckthorn lake paint followed by a glaze layer of copper resinate on top. Bone black in gum Arabic underdrawings were brushed on the substrate below the paint layers; b) FLIR SC7600 InSb camera direct image of the paint sample in the 1500-1650nm spectral range; c) FLIR SC7600 InSb camera direct image in the 1500-2500nm spectral range; d) 1960nm OCT 'en face' image through averaging those 'en face' layers with underdrawing signals. Image sizes are 7 mm by 10 mm.

5. Comparison of performance of supercontinuum and ASE sources in FDOCT

While supercontinuum generation provides an efficient means of producing broadband emission, it is difficult to produce emission with high temporal stability necessary for interferometric imaging requiring high fringe visibility. Superluminescent diodes (SLD) are commonly used in OCT systems owing to their low cost and low noise characteristics. Commercial supercontinuum sources in the 800 nm wavelength regime typically give OCT sensitivity that is 20-30 dB worse than those using semiconductor based ASE sources (SLDs). Recent work on generation of high quality, low noise supercontinuum sources have managed to reduce this noise penalty [18], however no such sources have yet been demonstrated in the 2000 nm wavelength regime.

In order to examine the temporal stability of the supercontinuum source described in this paper, we compare the difference between the OCT image quality and signal-to-noise ratio between this SC source and a previously built ASE light source. Using a FDOCT setup identical to that mentioned above, we first spectrally filtered the SC source such that the bandwidths were equal between the two sources (FWHM of 40 nm). The input power to the FDOCT was also adjusted to be equal for both cases (Fig. 6). The resulting A-scan profiles (Fig. 6b) of the FDOCT imaging of the same microscope coverslip using the two sources show a ~10 dB reduction in signal-to-noise for the supercontinuum source in comparison to the ASE source. A comparison of the B-Scan images of the paint sample shown in Fig. 4a gives the same impression qualitatively (Fig. 6c and 6d). The lower layers, in particular the smalt/chalk interface and the yellow ochre/chalk interface (c.f. Figure 4a) are much more visible in Fig. 6d than Fig. 6c. The chalk layer below the yellow ochre layer in the middle of the image around the boundary between smalt and yellow ochre paint (c.f. Figure 4a) is hardly visible in Fig. 6(c) but is clearly visible in Fig. 6(d).

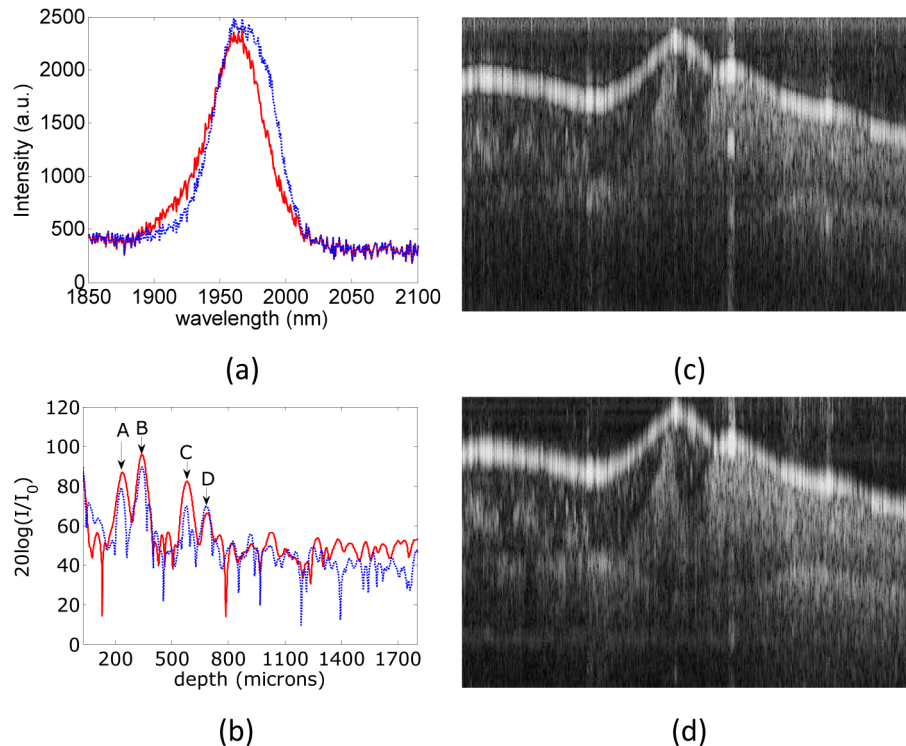


Fig. 6. a) Spectra of the SC source through a 40nm band pass filter (blue dotted) and the ASE source (red) reflected back from the reference arm; b) A-scan of a microscope coverslip using the two sources with the same FDOCT setup ('A' is the top air/coverslip interface, 'B' is the artefact due to interference between the top and the bottom of the coverslip, 'C' is the bottom of the coverslip, 'D' is the interference between the top of the coverslip and the 2nd reflection from the bottom of the coverslip after reflecting back once from the top interface); c) B-scan image of around the region of the paint sample in Fig. 4(a) marked in red using the SC source with the 40nm bandpass filter; d) same as c) but using the ASE source. The images in c) and d) are 7mm (width) by 0.8 mm (height).

6. Conclusions

A 1960 nm supercontinuum source has been developed with repetition rate between 10 kHz and 200 kHz and average power output of ~ 0.5 W. A spectrometer based Fourier domain OCT has been developed using the source at a repetition rate of 50 kHz (~ 100 ns pulse width and 220 nm bandwidth) to increase the depth of penetration in high opacity material with low water content. Specifically it has been demonstrated to improve depth of penetration through reduced scattering and absorption at longer wavelength for mock up samples of oil paintings. The broad bandwidth of the source resulted in a high axial resolution of $13 \mu\text{m}$ (in air) comparable to conventional OCT systems at shorter wavelengths such as 1300 nm. It is a significant improvement in axial resolution over our previous OCT setup with a 40 nm bandwidth ASE source. The Fourier domain setup with 2.5 kHz A-scan rate makes it at least an order of magnitude more efficient to capture 3D volume cubes and ~ 30 dB more sensitive compared with our previous time domain setup. The 1960 nm FDOCT described in this paper not only increases the probing depth but also has high enough resolution to resolve thin varnish and paint layers and is fast enough for efficient imaging of underdrawings over regions of a few centimeters in size. The application can be extended to other highly scattering material with low water content (e.g. teeth, bone) since Mie scattering reduces with increasing wavelength.

Acknowledgments

Funding from UK AHRC and EPSRC Science & Heritage Programme (Interdisciplinary Research Grant AH/H032665/1) is gratefully acknowledged. We are grateful to Nottingham Trent University for funding to purchase the FLIR InSb camera, the National Gallery for providing paint samples and Gooch & Housego plc. for providing the 2 μ m fiber couplers.